Ex-situ evaluation of PTFE coatedmetals in a proton exchangemembrane fuel cell environment

Olabi, Abdul-Ghani; Baroutaji, Ahmad; Carton, J.G.; Oladoye, Atinuke M. ; Stokes, Joseph; Twomey, B.

Published in:
Surface & Coatings Technology

DOI:
10.1016/j.surfcoat.2016.11.105

Published: 25/08/2017

Document Version
Peer reviewed version

Ex-Situ Evaluation of PTFE Coated Metals in a Proton Exchange Membrane Fuel Cell Environment

A. Baroutaji[1, 2*], J. G. Carton[1], A.M. Oladoye[1], J. Stokes[1], B. Twomey[3] and A.G. Olabi[4]

[1]Department of Mechanical and Manufacturing Engineering, Dublin City University, Dublin, Ireland

[2]Department of Process, Energy, and Transport Engineering, Cork Institute of Technology, Cork, Ireland

[3] EnBio Ltd., DCU Alpha Innovation Campus, Glasnevin Dublin 11, Ireland

[4]School of Engineering, University of the West of Scotland, Paisley, United Kingdom.

*Corresponding author: ahmad.baroutaji2@mail.dcu.ie

Abstract

Metallic-based bipolar plates exhibit several advantages over graphite-based plates, including higher strength, lower manufacturing cost and better electrical conductivity. However, poor corrosion resistance and high interfacial contact resistance (ICR) are major challenges for metallic bipolar plates used in proton exchange membrane (PEM) fuel cells.

Corrosion of metallic parts in PEM fuel cells not only increases the interfacial contact resistance but it can also decrease the proton conductivity of the Membrane Electrode Assembly (MEA), due to catalyst poisoning phenomena caused by corrosive products. In this paper, a composite coating of polytetrafluoroethylene (PTFE) was deposited on stainless steel alloys (SS304, SS316L) and Titanium (G-T2) via a CoBlast^{TM} process. Corrosion resistance of the coated and uncoated metals in a simulated PEM fuel cell environment of 0.5M H_2SO_4 + 2ppm HF at 70^{o}C was evaluated using potentiodynamic polarisation. ICR between the selected metals and carbon paper was measured and used as an indicator of surface conductivity. Scanning Electron Microscopy (SEM), 3D microscopy, Energy Dispersive X-ray (EDX), X-Ray Diffraction (XRD), and contact angle measurements were used to characterise the samples. The results showed that the PTFE coating improved the hydrophobicity and corrosion resistance but increased the ICR of the coated metals due to the unconductive nature of such coating. Thus, it was concluded that it is not fully feasible to use the PTFE alone for coating metals for fuel cell applications and a hybrid coating consisting of PTFE and a conductive material is needed to improve surface conductivity.

Keywords: PEM fuel cell; PTFE coatings; CoBlast^{TM}; Interfacial contact resistance; Flow plates; Corrosion.

1 Introduction

Proton exchange membrane (PEM) fuel cells are an attractive power source for a variety of mobile and stationary power applications due to their high efficiency, fast start-up, relative lightweight, low operating temperature and low environmental impact [1], [2]. Recently, PEM fuel cells have received an increased interest in the automobile sector as a potential alternative to the internal combustion engine [3]. However, in order to meet the full requirements of the automotive industry, the developers of PEM fuel cells have to address many essential issues related to cost, operation and durability of fuel cell components, particularly in comparison with internal combustion engines. One of the key strategies for improving the performance and durability, while reducing the cost of the PEM fuel cell, is to design and develop low-cost bipolar plates with high corrosion resistance and surface conductivity [4]–[7].

Bipolar plates are key components of a PEM fuel cell stack and perform vital roles such as distributing the fuel and oxidant to the catalyst layer, removing the water from the fuel cell and collecting the produced current [8]. Traditionally, bipolar plates are fabricated from graphite due to its high corrosion resistance, relatively low surface contact resistance and high surface conductivity in the PEM fuel cell environments. However, graphite is brittle, permeable to gases, and expensive to mass produce. Thus, metals and carbon-based composites have been considered to develop cost-effective and durable bipolar plates that can replace graphite. Metals and their alloys provide several advantages over the carbon-based materials, as they possess higher mechanical strength, can be made thinner to achieve higher power density, are more durable, not permeable, and have higher cost effectiveness, with respect to mass production. However, metals considered for bipolar applications are prone to corrosion and exhibit high contact resistance in PEM fuel cell environments (pH=2-3 at ~ 70°C) [9]. The dissolved metal ions, generated from corrosion, can poison the active sites of the membrane electrode assembly (MEA) resulting in decreased power output of the fuel cell [10], [11]. Furthermore, these metals develop a passive oxide layer that increases ICR [12].

Therefore, a considerable amount of research has investigated the corrosion behaviour of metal alloys such as stainless steel (SS) [11], [13]–[18], titanium (Ti) [19]–[21], and

aluminium (Al) [22], [23]. SS alloys have been considered as the reference materials for metal bipolar plates [11], [24]–[26]. The performance of SS in the PEM fuel cell environment is strongly depended on alloying elements such as Cr, Ni and Mo [25], [26]. The SS alloys with higher Cr and Ni content exhibit thinner oxide layer resulting in lower ICR which make such alloys recommended for bipolar plate applications [25]. Ti and its alloys were also considered as a suitable material for bipolar plate applications due to its high strength to weight ratio and also its outstanding chemical stability in acidic environments. It was indicated through many investigations that uncoated Ti has better anti-corrosion properties than the uncoated SS316 in PEM fuel cell environments, but the power output was lower due to the thicker oxide formed on the surface of Ti and the released ions such as Ti^{+2} [19], [25], [27]. Al and its alloys are attractive metals for metallic bipolar plates due to low density, cost effectiveness and ease of fabrication features [28]. However, Al and its alloys are not as good as SS and Ti due to its higher corrosion rate and shorter life.

To overcome the corrosion and high ICR problems, significant research efforts have been directed into improving the corrosion resistance via surface modifications. Surface coatings/treatments for metallic bipolar plates applications are mainly divided into: carbon-based and metal based coatings [29]–[31]. Carbon-based coatings include conductive polymers, graphite and composite coatings [1], [8]. The metal-base coatings for bipolar plate applications include noble metals, metal nitrides, metal carbides, and conductive metal oxides [1], [8]. Whilst some of these coatings e.g. metal nitrides have been extensively investigated; studies on other coatings such as PTFE are relatively rare. The PTFE coating is well known for its potentials to improve the hydrophilicity of the bipolar plates that in turn allows for better water management and reduce the mass transport loses of the PEM fuel cell [32]. Fu et al [32] reported on the performance of Ag–PTFE composite coating on 316L stainless steel used as bipolar plate of PEM fuel cell. It was found that the PTFE has a significant influence on the hydrophobic characteristics of SS, as a greater contact angle was observed in the PTFE-coated surface, which implies better hydrophobicity. Similar observations were reported by Show et al [33] who described that the contact angle of SS increased from 60^{o} to 110^{o} upon using the PTFE coating. Show and Takahashi [34] reported on the ex-situ and in-situ performance of carbon nanotube (CNT)/PTFE composite film. It was found that using of CNT/PTFE coating on SS improved corrosion resistance and increased the lifetime of the fuel cell.

Overall, PTFE coating has received very limited attention for PEM fuel cell bipolar plate application. Therefore, in this paper, we explore the suitability of PTFE-coated stainless steel and titanium for use in a PEM fuel cell environment. The PTFE coating is deposited on metals using a powder coating processes named CoBlast^{TM} process. The suitability of such a coating for corrosion protection and surface conductivity in simulated a PEM fuel cell environment is evaluated via electrochemical polarisation and interfacial contact resistance (ICR) techniques, respectively.

2 Experiment

2.1 Materials and coatings

In this study, titanium G2 and stainless steel type 316L and 304 were selected as metallic substrates. The coating powder consisted of a blend of PTFE powder (Zonyl^{TM}, Dupont, USA) and alumina powder (particles size: 50 µm; Comco Inc., CA, USA) mixed in a predefined ratio in a laboratory turbula for fifteen minutes. Alumina facilitates removal of the surface oxide in order for the coating powder (PTFE) to be impregnated onto the metal surface by tribo chemical bonding and mechanical interlocking [35]–[37]. Table 1 summarises the metals investigated and their respective designation.

2.2 Deposition Process

Prior to deposition, the various substrates were thoroughly wiped with isopropanol, air dried and arranged on the platform of the CoBlast^{TM} coating equipment at a working distance of 20 mm from the CoBlast^{TM} nozzle head. The metal surfaces were thereafter modified by blasting with streams of the processed powder fed through the CoBlast^{TM} nozzle at 90 psi and speed of 12 mm/s [35]. The blasting process was continued in the perpendicular direction until the entire surface was covered. After coating, the modified surfaces were blasted with dry air to remove loosely adhered material and washed with isopropanol.

2.3 Characterisation

2.3.1 Surface characterisation

Surface morphologies of the samples were examined with a bench top ZEISS EVOLS 15 SEM operated at 15kV accelerating voltage in the secondary and backscattered electron mode while compositional analysis of the samples was obtained using EDX (INCA, Oxford instruments).

Surface microscopy was conducted with a VHX-2000 digital microscope (Keyence, USA). Images were taken using the 500X lens and 3D imaging permitted a sharp depth of field.

XRD analysis was conducted with a D8 Advance Bruker X-ray diffractometer with CuKα radiation anode source operated at accelerating voltage of 40 kV and beam current of 40 mA in the 10°– 80° range.

A surface roughness tester TR-200, (CV Instruments Europe, UK) was used to measure the surface roughness of the samples pre and post coating. Values of 5mm, 0.8mm and 0.01μm were selected for the cut-off length, step and resolution respectively. The test was repeated three times for each sample. R_a and R_q values were recorded in each test and the mean values were calculated.

2.3.2 Contact angle measurements

Water contact angle measurements were conducted with a FTA200 (First Ten Angstroms, Portsmouth, USA) contact angle analyser. A predefined volume of distilled water was dropped on the surfaces of the sample via a computer controlled syringe pump. Images of the water drop on the surface of the samples were captured and then analysed with the FTA32 Video 2.0 software. Mean values for three measurements are reported.

2.3.3 Interfacial contact resistance

ICR between the different samples and carbon paper was evaluated by a method previously described by Wang et al [11]. The setup consisted of two pieces of Toray Teflon treated carbon paper (TGP-H-090, Fuel Cell Store, US) sandwiched between the coated samples and two copper electrodes. A direct current of 1 A was supplied to the copper electrode via a XHR 300-3.5DC power source. The voltage drop across the setup was measured with Tektronix DMM912 digital multi-meter while gradually applying compressive forces with a Zwick Roell (Z5 kN) ultimate tensile strength machine. The total resistance of the setup was calculated based on Ohm's law (R=V/I) with correction made for the resistance of the carbon paper/copper interfaces. The ICR can be calculated as follows:

$$2 \times ICR = A \times (R - R_{cp}) \qquad \text{Equation. 1}$$

where A is the surface area of the sample, R_{cp} is the resistance of the interface between the carbon paper and copper electrode, R is the overall resistance of all interfaces including carbon paper/copper electrode interface and copper electrode/tested sample interface.

2.3.4 Electrochemical polarisation

The electrochemical test setup used for evaluating the corrosion behaviour of the samples consisted of a flat corrosion cell (Princeton Applied Research, K0235, USA) in which the working electrode (coated and uncoated metal samples) are pressed against a Teflon "O" ring exposing 1 cm^2 of the working electrode to the electrolyte, 0.5M H_2SO_4 + 2ppm HF with an Ag/AgCl (saturated KCl) as the reference electrode and a platinum mesh as the counter electrode. The setup was connected to a Gamry Interface 1000 (Scientific & Medical Products Limited, UK) potentiostat. Potentiodynamic scans were conducted at 70° C. Prior to and during the polarisation experiments, the electrolyte was bubbled thoroughly with pressurised air or hydrogen to depict the PEM fuel cell cathodic and anodic environments respectively while the open circuit potential (OCP) was measured for 15 minutes. Potentiodynamic scans were conducted at a scan rate of 1 mV/s from −1 V vs.OCP to 1 V vs. reference.

3 Results and discussion

3.1 Surface characterisation

Figure 1 displays the surface morphologies of uncoated and coated metals. The SEM image revealed a surface topography indicating the presence of metal peaks throughout the surface as a result of the combined abrasive and plastic deformation effects of CoBlast, however the CoBlast process does not provide 100% coating coverage [26]. The roughness profile as shown in Table 2 confirms the roughness increase caused by the CoBlast process.

Figure 2 shows the X-ray diffraction pattern of the coated and uncoated materials respectively. The XRD patterns for all coated metals confirmed the presence of PTFE on the near surface characterised with a peak at 18.9^o. Also, low intense peaks of alumina, which originated from the grit material in the abrasive powder used in the CoBlast process, can be observed as well as that for peaks of the substrates.

Figure 3 shows an optical comparison of coated and uncoated samples before and after the polarisation tests. It is identified that most uncoated samples, exhibited surface degradation evidenced by the roughening and darkening of the surface and the emergence of pits on the substrates. The SS316L sample did not show surface degradation but became slightly brighter post polarisation testing. The PTFE coated samples, identified with a white covering on the surface, are seen to have less evidence of pitting but they have darkened in most cases,

indicating that the surface was not fully coated. SS316L here also exhibited a brighter surface due to the exposure to the acidic environment.

3.2 Contact angle

The photographs of a water droplet on the surfaces of coated and uncoated metals along with the mean value of contact angles with water (φ) are shown in Figure 4. The contact angles of the different samples are 76.44^{o}, 130.84^{o}, 70.31^{o}, 128.67^{o}, 83.85^{o}, 127.45^{o} for TIG2, CTIG2, SS316L, CSS316L, SS304, CSS304, respectively. It is clear that the contact angles of the PTFE-coated samples are greater than the uncoated counterparts. This is a proof that the PTFE coating can alter the surface of metals from hydrophilic to hydrophobic nature. The improved hydrophobic characteristic of the PTFE-coated bipolar plate enables better water removals and stabilises the electric output of the fuel cell.

3.3 Interfacial contact resistance

The values of interfacial contact resistance for the coated and uncoated samples were measured to get a depth understanding of the impact of coating on internal impedance of the fuel cell. The variations of ICR with the compaction force of uncoated and coated samples are shown in Figure 5 for SS316L, SS304, and TiG2 respectively. It is clear from this figure that the ICR decreased as the compaction force increased for coated and uncoated samples. A rapid decrease in ICR values was observed at low compaction force followed by a gradual stability at a certain value. This is due to the fact that at low compaction force, the carbon paper (GDL layer) comes in contact with the lower area on the surface of sample. As the compaction force increases, the contact area between carbon paper and coating surface increases until a maximum value is reached where no further increase in effective contact area can be noticed, similar observation was also reported by Tian et al [38].

Uncoated grit-blasted (GB) and polished (PO) samples, used for comparison, offer similar behaviour in terms of ICR for samples under investigation. However, the coated samples exhibited higher values of contact resistance in comparison with uncoated samples. This behaviour may be attributed to the low electrical conductivity of the PTFE coating that leads to higher electric resistance in the coated samples. Also, the surface roughness of the samples has a profound effect on the value of ICR where the higher surface roughness leads to higher ICR [39]. As seen from Table 2, the coated samples have higher surface roughness than the uncoated samples, and thus higher ICR values were reported for coated samples. However, the ICR values of coated samples come close to that of uncoated samples at compaction forces of 40-50 N.cm^{-2}.

A comparison of ICR values for coated and uncoated samples at compaction force of 50 $N.cm^{-2}$ is presented in Figure 6. Lower ICR values were obtained for TIG2 samples while both stainless steel samples showed similar ICR values. It is confirmed that the coated samples have higher ICR values when compared to uncoated samples.

3.4 Electrochemical polarisation

Figure 7 presents the potentiodynamic polarisation curves obtained for coated and uncoated substrates exposed to 0.5M H_2SO_4 + 2ppm HF at 70° C. Air and hydrogen gas were bubbled into the electrolyte to simulate the PEM fuel cell cathode and anode environments respectively. Table 3 shows the corrosion parameters for the materials. Comparing these parameters, it can be seen that in the simulated cathode environment, all PTFE coated stainless steel samples exhibited higher corrosion potentials (E_{corr}) values and similar corrosion current density (I_{corr}). This confirms that the PTFE coating can slightly improve the corrosion protection of stainless steel in the simulated cathode PEM fuel cell environment. For the TiG2 samples, on the other hand, the PTFE coated samples exhibited similar E_{corr} values with the substrate, but a higher I_{corr}. This indicates that the corrosion resistance of the TiG2 substrate was not improved in the cathodic environment. It was noticed that in the simulated anodic environment, all PTFE coated samples exhibited higher corrosion resistance than the substrate, evidenced by a higher E_{corr} value and a decrease in I_{corr} of the samples. The higher E_{corr} values, observed with the coated samples, decreases the corrosion tendency of the PTFE coated samples in the simulated anodic environment of the PEM fuel cell. At the same time, a lower I_{corr} implies that the corrosion rate of these samples was reduced to some extent. The enhanced corrosion resistance of the PTFE coated samples, under the simulated anodic environment is certainly related to the loss of passivity by the substrate in such an environment.

4 Conclusion

PTFE coated metals were investigated for the first time for their suitability to fabricate PEM fuel cell bipolar plates. The corrosion and conductivity behaviour of PTFE coated stainless steel and titanium substrates have been analysed and characterised. CoBlast^{TM} process was used to deposit a PTFE coating on the metal substrates. Contact angle measurements were conducted and showed a noticeable improvement in the hydrophobic property of the PTFE-treated surfaces which is greatly beneficial for the water management in PEM fuel cell. ICR was measured for all samples to examine the effect of the coating layer on the conductivity of

metal. Higher ICR values were observed for the coated samples, due to higher surface roughness and lower electrical conductivity of the PTFE coated samples. It is considered that the conductivity behaviour of such coated samples may be improved by adding a conductive material to PTFE such as silver (Ag). The corrosion current density and corrosion potential of the PTFE coated samples in a simulated anodic and cathodic PEMFC environment of 0.5M H_2SO_4 + 2ppm HF at 70°C were investigated. The results showed that, in the cathodic environment, the corrosion resistance of PTFE coated stainless steel substrates was slightly improved while no improvement was noticed for TiG2 substrate. On the other hand, the corrosion resistance of all coated samples was enhanced in the anodic environment and this may be due to the loss of passivity in this environment.

Acknowledgement

The authors would like to thank Enterprise Ireland for funding this work under grant CF20133023.

5 References

[1] A. Baroutaji, J. G. Carton, M. Sajjia, and A. G. Olabi, "Materials in PEM Fuel Cells," in *Reference Module in Materials Science and Materials Engineering*, Elsevier, 2016.

[2] A. Alaswad, A. Baroutaji, H. Achour, J. Carton, and A. Al Makky, "Developments in fuel cell technologies in the transport sector," *Int. J. Hydrogen Energy*, vol. 41, no. 37, pp. 16499–16508, 2016.

[3] "FUEL CELLS." [Online]. Available: http://energy.gov/eere/fuelcells/fuel-cells. [Accessed: 30-Jun-2016].

[4] A. Baroutaji, J. Carton, J. Stokes, and A.-G. Olabi, "Design and development of proton exchange membrane fuel cell using open pore cellular foam as flow plate material," *Journal of Energy Challenges and Mechanics*. North Sea Conference & Journal LTD, 06-Sep-2014.

[5] J. G. Carton and A. G. Olabi, "Three-dimensional proton exchange membrane fuel cell model: Comparison of double channel and open pore cellular foam flow plates," *Energy*, 2016.

[6] J. G. Carton and A. Baroutaji, "Developments of Foam Materials for Fuel Cell Technology," in *Reference Module in Materials Science and Materials Engineering*, Elsevier, 2016.

[7] J. G. Carton and A. G. Olabi, "Representative model and flow characteristics of open pore cellular foam and potential use in proton exchange membrane fuel cells," *Int. J. Hydrogen Energy*, vol. 40, no. 16, pp. 5726–5738, May 2015.

[8] P. J. Hamilton and B. G. Pollet, "Polymer Electrolyte Membrane Fuel Cell (PEMFC) Flow Field Plate: Design, Materials and Characterisation," *Fuel Cells*, vol. 10, no. 4, pp. 489–509, May 2010.

[9] A. HERMANN, T. CHAUDHURI, and P. SPAGNOL, "Bipolar plates for PEM fuel cells: A review," *Int. J. Hydrogen Energy*, vol. 30, no. 12, pp. 1297–1302, Sep. 2005.

[10] A. Pozio, R. F. Silva, M. De Francesco, and L. Giorgi, "Nafion degradation in PEFCs from end plate iron contamination," *Electrochim. Acta*, vol. 48, no. 11, pp. 1543–1549, May 2003.

[11] H. Wang, "Stainless steel as bipolar plate material for polymer electrolyte membrane fuel cells," *J. Power Sources*, vol. 115, no. 2, pp. 243–251, Apr. 2003.

[12] R. A. Antunes, M. C. L. Oliveira, G. Ett, and V. Ett, "Corrosion of metal bipolar plates for PEM fuel cells: A review," *Int. J. Hydrogen Energy*, vol. 35, no. 8, pp. 3632–3647,

Apr. 2010.

[13] K. Feng, Z. Li, X. Cai, and P. K. Chu, “Corrosion behavior and electrical conductivity of niobium implanted 316L stainless steel used as bipolar plates in polymer electrolyte membrane fuel cells,” *Surf. Coatings Technol.*, vol. 205, no. 1, pp. 85–91, 2010.

[14] O. Lavigne, C. Alemany-Dumont, B. Normand, P. Delichère, and A. Descamps, “Cerium insertion in 316L passive film: Effect on conductivity and corrosion resistance performances of metallic bipolar plates for PEM fuel cell application,” *Surf. Coatings Technol.*, vol. 205, no. 7, pp. 1870–1877, 2010.

[15] N. Mohammadi, M. Yari, and S. R. Allahkaram, “Characterization of PbO2 coating electrodeposited onto stainless steel 316L substrate for using as PEMFC’s bipolar plates,” *Surf. Coatings Technol.*, vol. 236, pp. 341–346, 2013.

[16] K. Lin, X. Li, L. Tian, and H. Dong, “Active screen plasma surface co-alloying treatments of 316 stainless steel with nitrogen and silver for fuel cell bipolar plates,” *Surf. Coatings Technol.*, vol. 283, pp. 122–128, 2015.

[17] Z. Wang, Y. Wang, Z. Li, K. Feng, J. Huang, F. Lu, C. Yao, X. Cai, and Y. Wu, “Investigation of C/Al–Cr–N multilayer coatings for stainless steel bipolar plate in polymer electrolyte membrane fuel cells,” *Surf. Coatings Technol.*, vol. 258, pp. 1068–1074, 2014.

[18] A. M. Oladoye, J. G. Carton, K. Benyounis, J. Stokes, and A. G. Olabi, “Optimisation of pack chromised stainless steel for proton exchange membrane fuel cells bipolar plates using response surface methodology,” *Surf. Coatings Technol.*, vol. 304, pp. 384–392, 2016.

[19] Y. Wang and D. Northwood, “An Investigation of Commercial Grade 2 Titanium as a Bipolar Plate Material for PEM Fuel Cells,” in *ECS Transactions*, 2008, vol. 11, no. 18, pp. 53–60.

[20] Y. Soma, I. Muto, and N. Hara, “Electrochemical Properties of Titanium in PEFC Bipolar Plate Environments,” *Mater. Trans.*, vol. 51, no. 5, pp. 939–947, Apr. 2010.

[21] A. M. Oladoye, J. G. Carton, and A. G. Olabi, “Evaluation of CoBlast Coated Titanium Alloy as Proton Exchange Membrane Fuel Cell Bipolar Plates,” *J. Mater.*, vol. 2014, pp. 1–10, 2014.

[22] S. A. A. El-Enin, O. E. Abdel-Salam, H. El-Abd, and A. M. Amin, “New electroplated aluminum bipolar plate for PEM fuel cell,” *J. Power Sources*, vol. 177, no. 1, pp. 131–136, Feb. 2008.

[23] Y. Hung, K. M. El-Khatib, and H. Tawfik, “Testing and evaluation of aluminum

coated bipolar plates of pem fuel cells operating at 70°C," *J. Power Sources*, vol. 163, no. 1, pp. 509–513, Dec. 2006.

[24] Y. Wang and D. O. Northwood, "Effects of O2 and H2 on the corrosion of SS316L metallic bipolar plate materials in simulated anode and cathode environments of PEM fuel cells," *Electrochim. Acta*, vol. 52, no. 24, pp. 6793–6798, Aug. 2007.

[25] D. P. Davies, P. L. Adcock, M. Turpin, and S. J. Rowen, "Bipolar plate materials for solid polymer fuel cells," *J. Appl. Electrochem.*, vol. 30, no. 1, pp. 101–105, 2000.

[26] H. Wang and J. A. Turner, "Ferritic stainless steels as bipolar plate material for polymer electrolyte membrane fuel cells," *J. Power Sources*, vol. 128, no. 2, pp. 193–200, Apr. 2004.

[27] L. Ma, S. Warthesen, and D. A. Shores, "Evaluation of materials for bipolar plates in PEMFCs - JNMES - Journal of New Materials for Electrochemical Systems," *J. New Mater. Electrochem. Syst.*, vol. 3, pp. 221–228, 2000.

[28] H. Deng, X. Zhang, Z. Ma, H. Chen, Q. Sun, Y. Zhang, and X. Liu, "A micro passive direct methanol fuel cell with high performance via plasma electrolytic oxidation on aluminum-based substrate," *Energy*, vol. 78, pp. 149–153, 2014.

[29] R. L. Borup and N. E. Vanderborgh, "Design and Testing Criteria for Bipolar Plate Materials for Pem Fuel Cell Applications," *MRS Proc.*, vol. 393, p. 151, Feb. 2011.

[30] V. Mehta and J. S. Cooper, "Review and analysis of PEM fuel cell design and manufacturing," *J. Power Sources*, vol. 114, no. 1, pp. 32–53, Feb. 2003.

[31] M. C. Kimble, A. S. Woodman, and E. B. Anderson, "American Electroplaters and Surface Finishers Society 1999," in *AESF SUR/FIN*, 1999, vol. 99, pp. 21–24.

[32] Y. Fu, M. Hou, H. Xu, Z. Hou, P. Ming, Z. Shao, and B. Yi, "Ag–polytetrafluoroethylene composite coating on stainless steel as bipolar plate of proton exchange membrane fuel cell," *J. Power Sources*, vol. 182, no. 2, pp. 580–584, Aug. 2008.

[33] Y. Show, T. Nakashima, Y. Fukami, Y. Show, T. Nakashima, and Y. Fukami, "Anticorrosion Coating of Carbon Nanotube/Polytetrafluoroethylene Composite Film on the Stainless Steel Bipolar Plate for Proton Exchange Membrane Fuel Cells," *J. Nanomater.*, vol. 2013, pp. 1–7, 2013.

[34] Y. Show and K. Takahashi, "Stainless steel bipolar plate coated with carbon nanotube (CNT)/polytetrafluoroethylene (PTFE) composite film for proton exchange membrane fuel cell (PEMFC)," 2009.

[35] L. O'Neill, C. O'Sullivan, P. O'Hare, L. Sexton, F. Keady, and J. O'Donoghue,

"Deposition of substituted apatites onto titanium surfaces using a novel blasting process," *Surf. Coatings Technol.*, vol. 204, no. 4, pp. 484–488, 2009.

[36] P. Sullivan and N. D. Hare, "C. O'O'O'Leary , 'Deposition of substituted apatites with anticolonizing properties onto titanium surfaces using a novel blasting process,' Journal of Biomedical Materials Research—Biomaterials, vol. no. 1, pp. , .," vol. 95 SRC-, pp. 141–149, 2010.

[37] A. M. Oladoye, J. G. Carton, and A. G. Olabi, "Characterization of Graphite Coatings Produced by CoBlast™ Technology," *JOM*, vol. 66, no. 4, pp. 602–607, Apr. 2014.

[38] R. J. Tian, J. C. Sun, and L. Wang, "Effect of plasma nitriding on behavior of austenitic stainless steel 304L bipolar plate in proton exchange membrane fuel cell," 2007.

[39] B. Avasarala and P. Haldar, "Effect of surface roughness of composite bipolar plates on the contact resistance of a proton exchange membrane fuel cell," 2009.

Figure 1 Topographical view of the coated and uncoated samples.

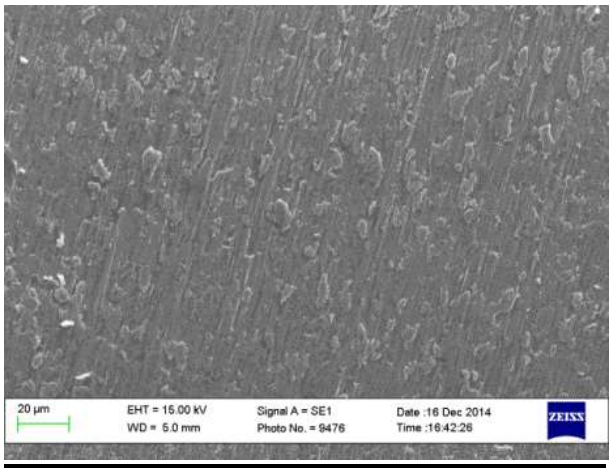

Ti

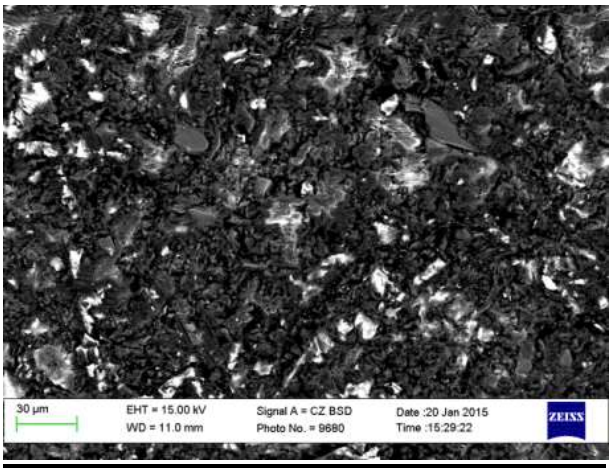

CTiG2

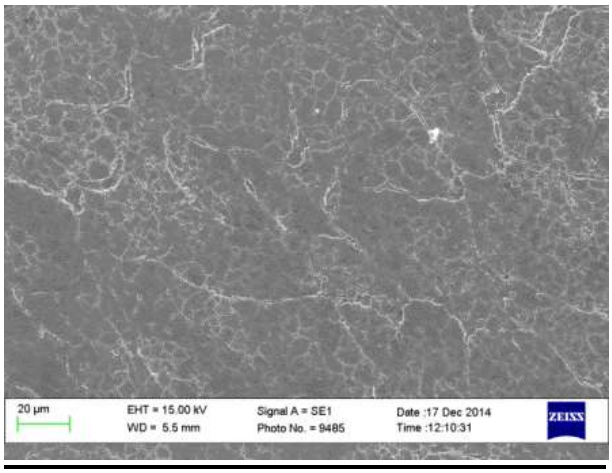

SS316L

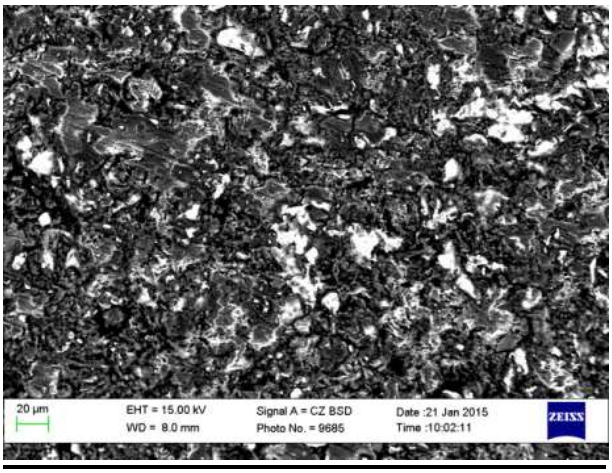

CSS316L

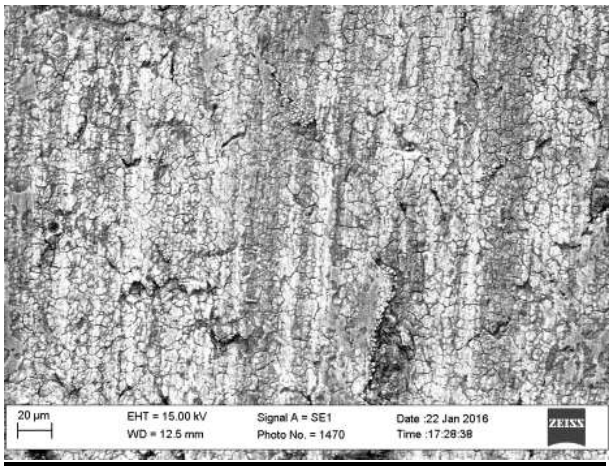

SS304

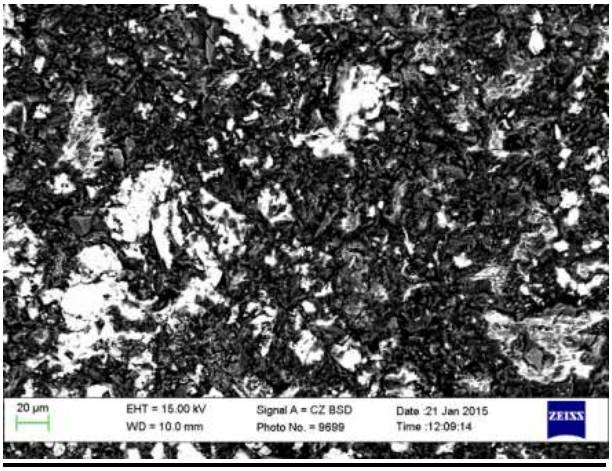

CSS304

Figure 2: XRD analysis of (a) Ti, (b) SS samples

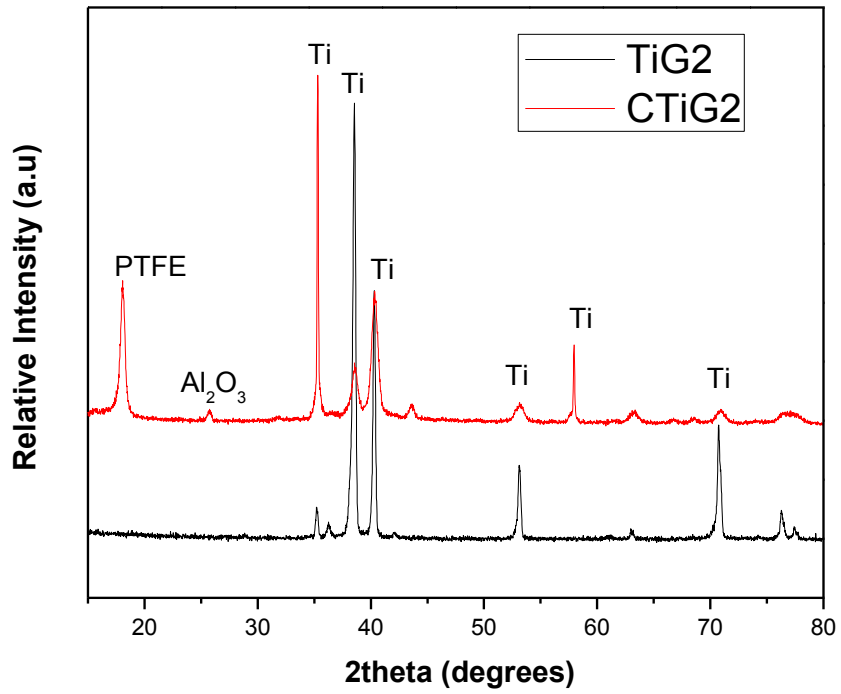

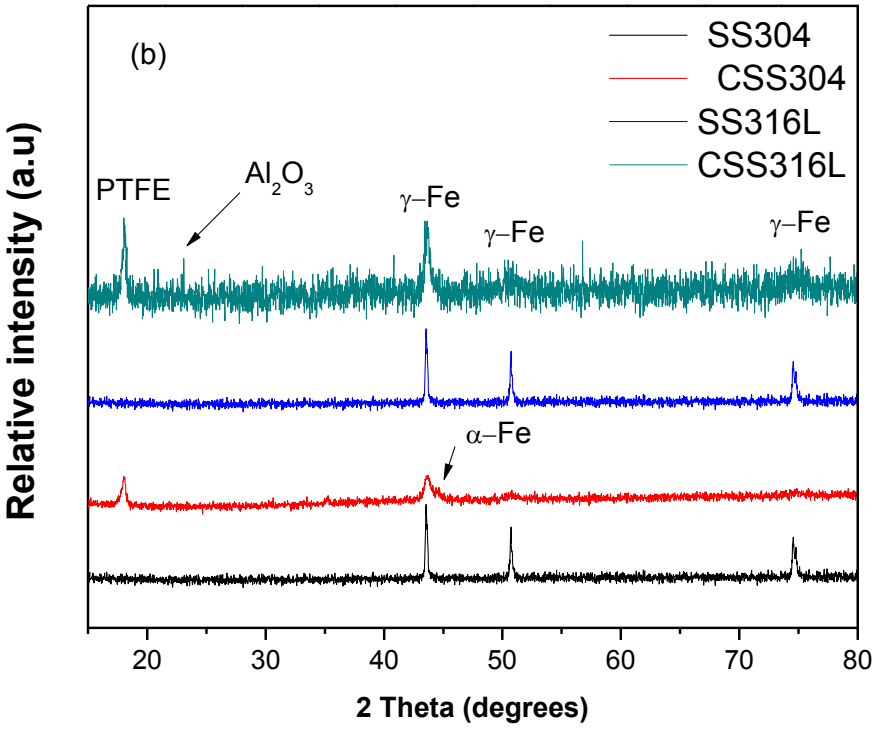

Figure 3 Optical images of coated and uncoated samples.

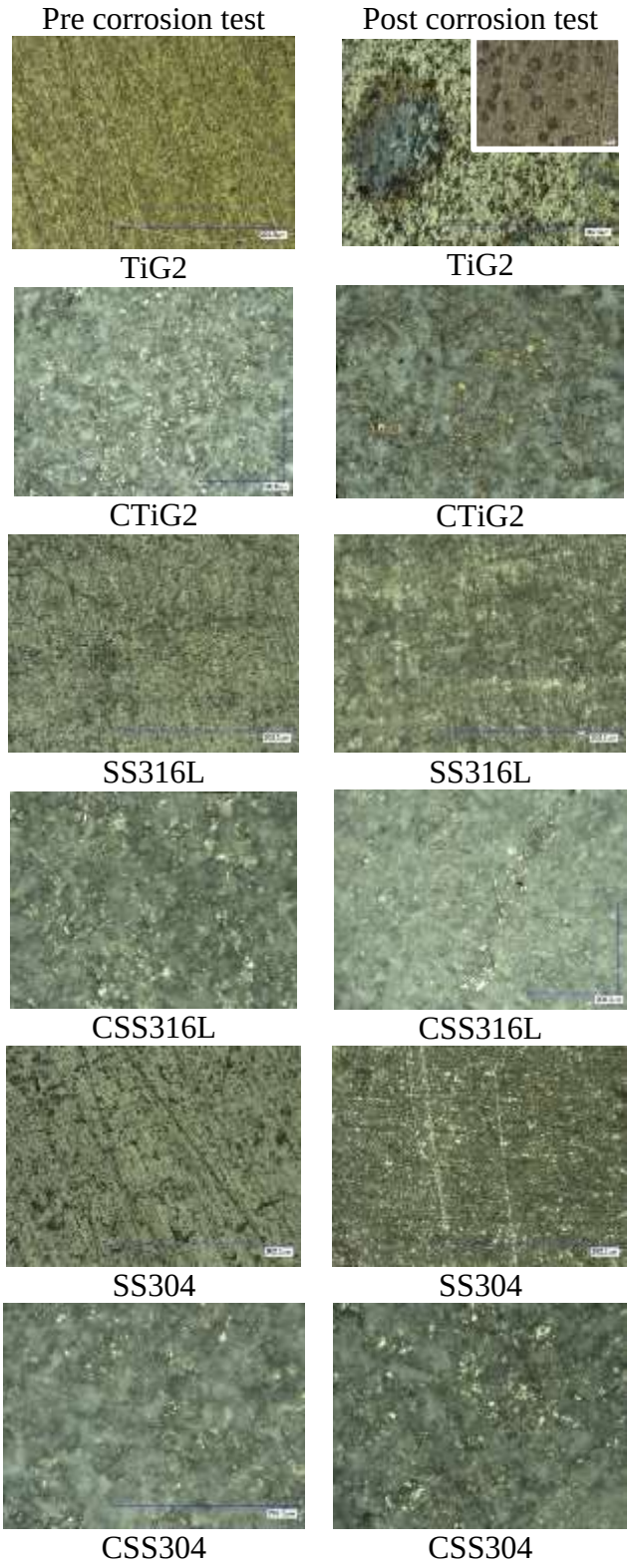

Figure 4: Water contact angels of coated and uncoated metals

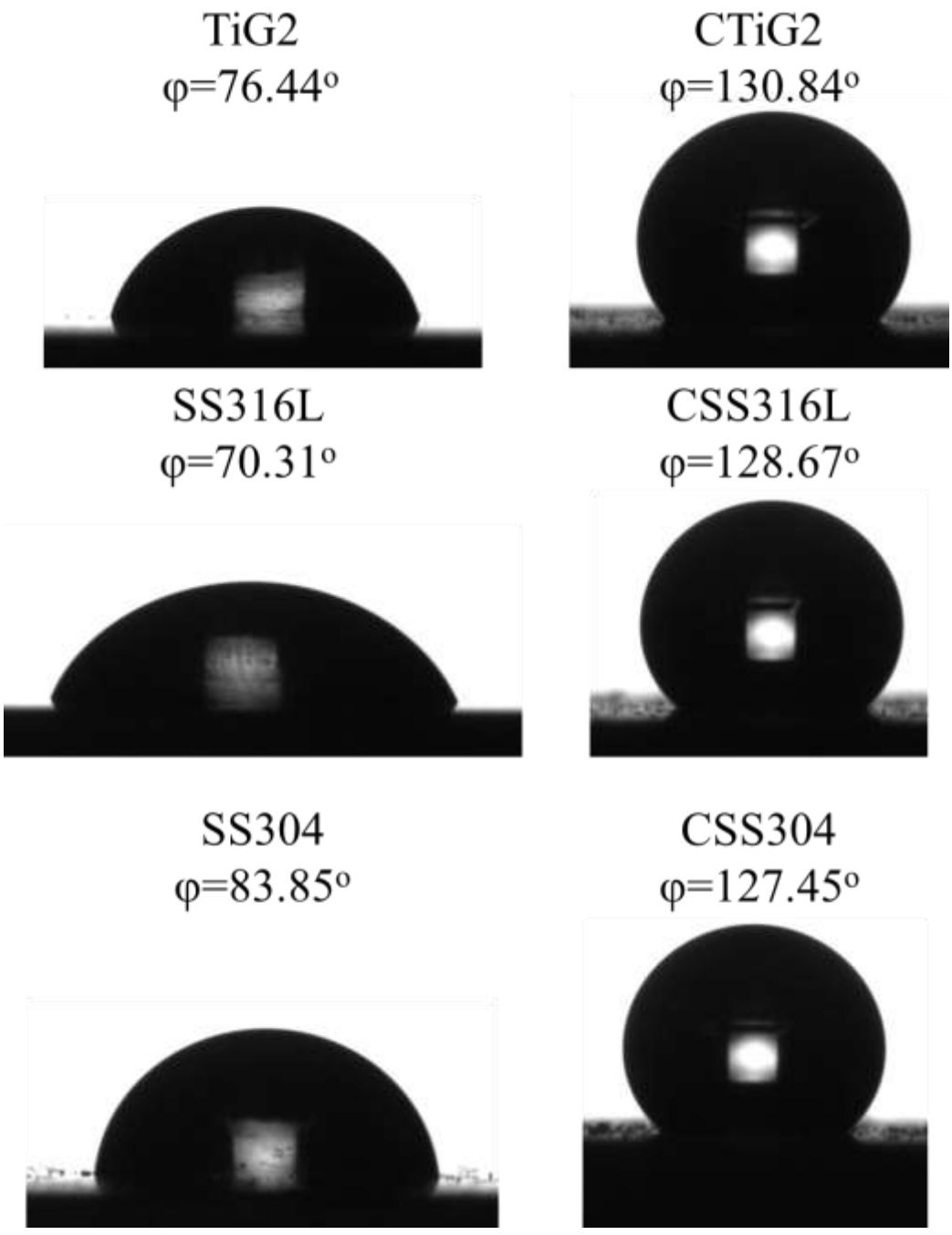

Figure 5: Variation of ICR with compaction force of uncoated and coated (a) TIG2 (b) SS316L (c) SS304

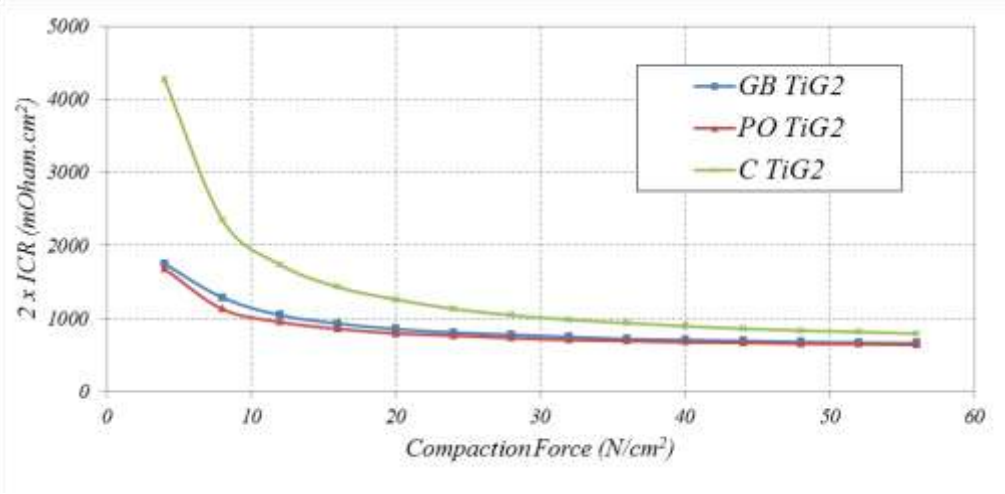

(a)

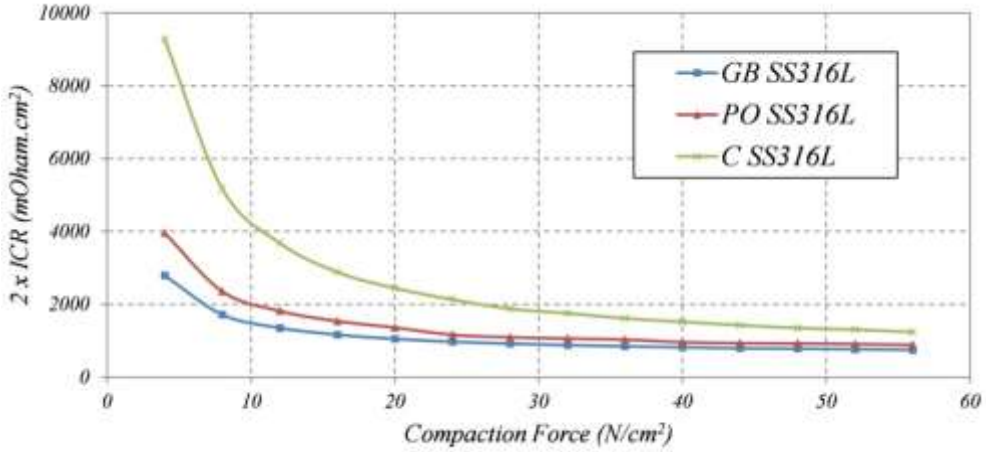

(b)

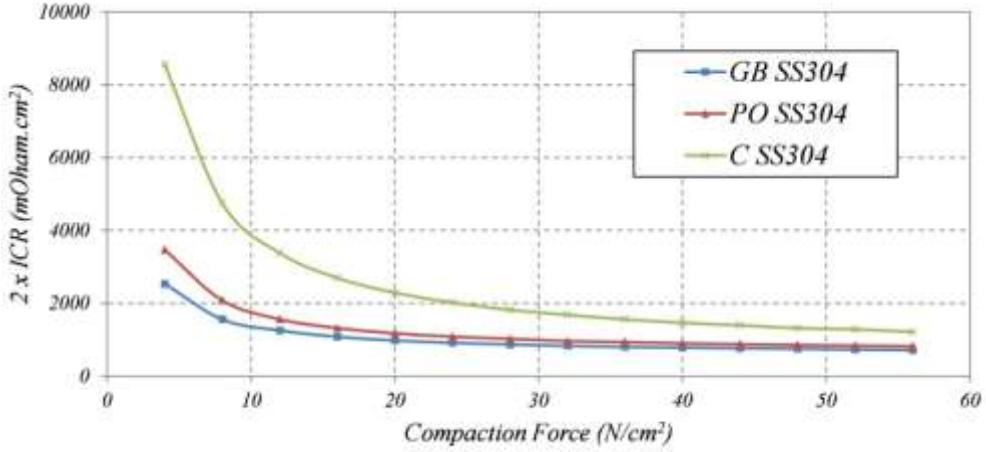

(c)

Figure 6: Comparison of ICR values at compaction force of 50 N.cm^{-2}

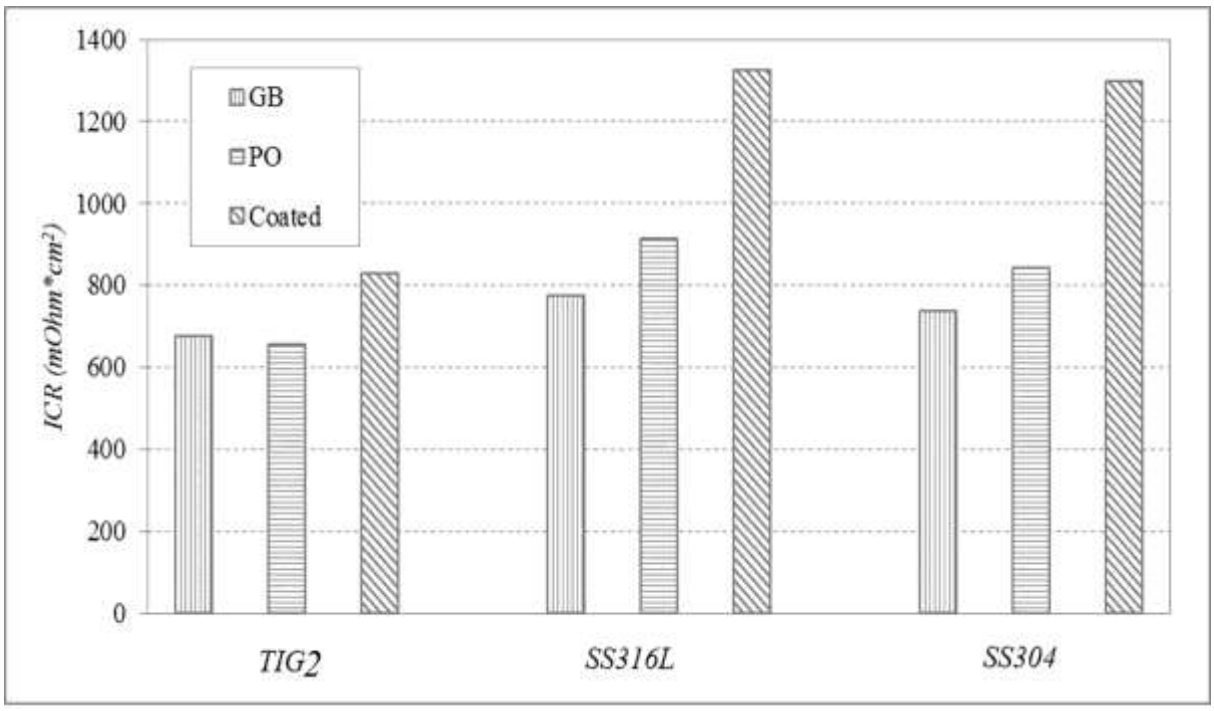

Figure 7: Potentiodynamic polarisation curves of PTFE coated and uncoated samples exposed to 0.5M H_2SO_4 +2ppm HF at 70^o C under (a) cathodic (b) anodic PEMFC conditions

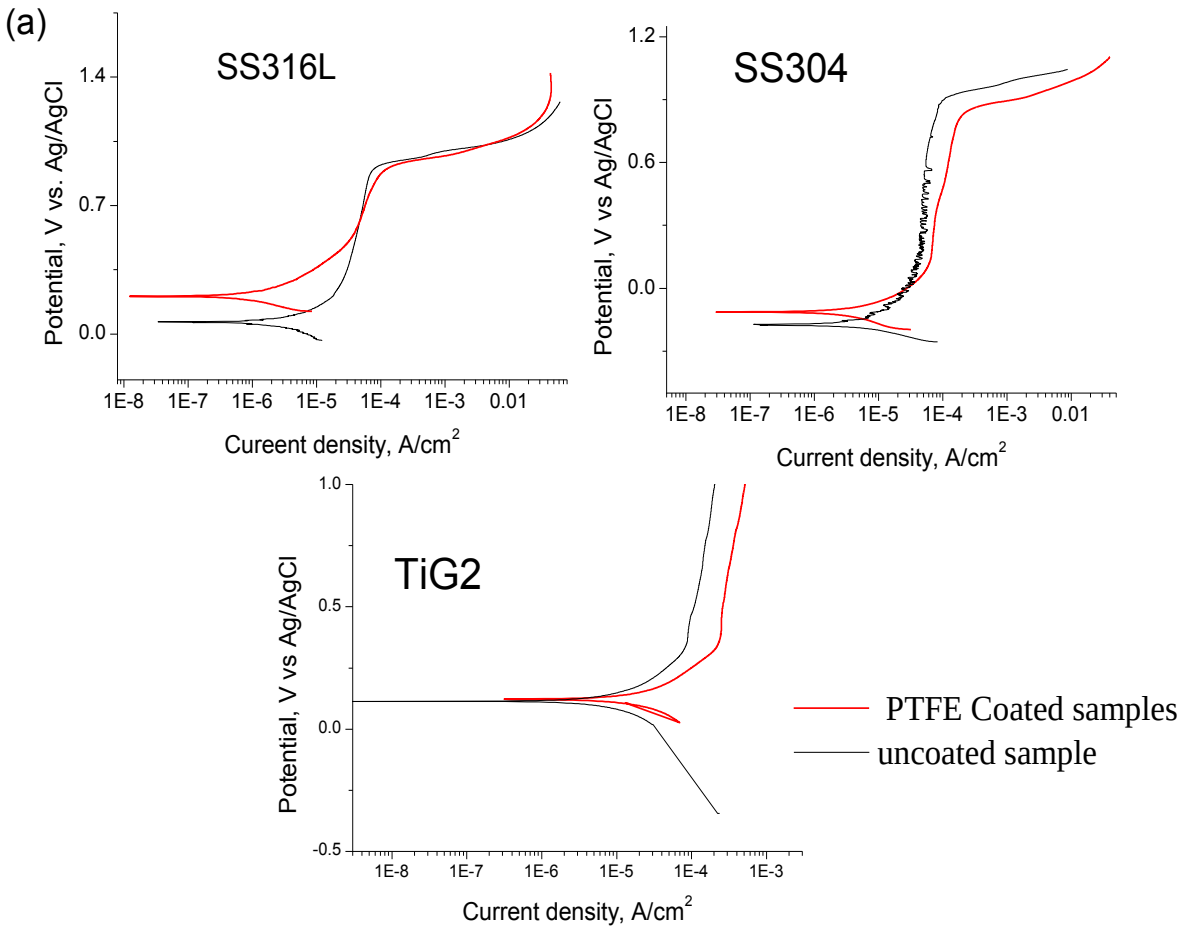

(b)

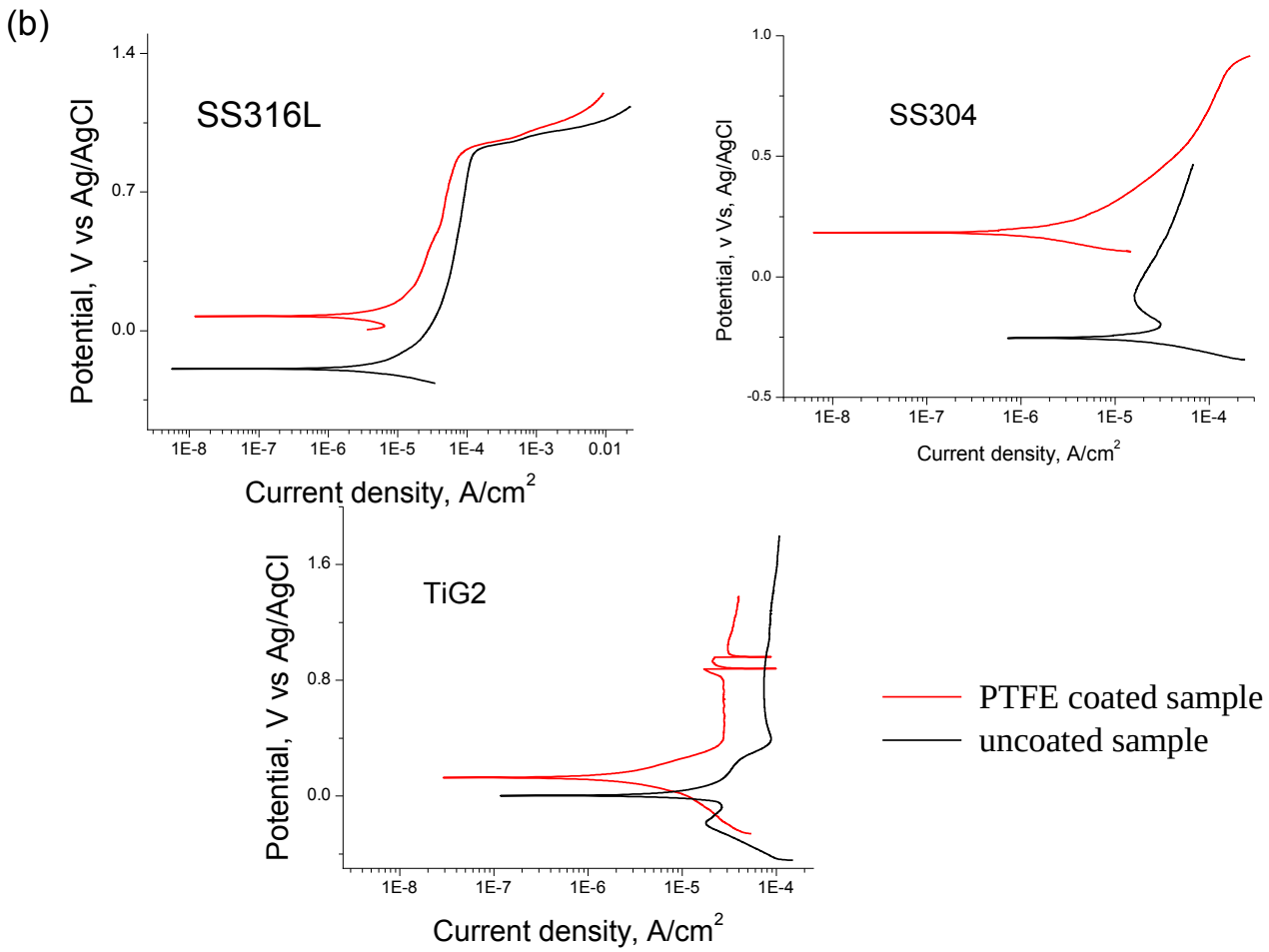
SS316L
Potential, V vs Ag/AgCl
1.4
0.7
0.0
1E-8
1E-7
1E-6
1E-5
1E-4
1E-3
0.01
Current density, A/cm2
SS304
Potential, v Vs, Ag/AgCl
1.0
0.5
0.0
-0.5
1E-8
1E-7
1E-6
1E-5
1E-4
Current density, A/cm2
TiG2
Potential, V vs Ag/AgCl
1.6
0.8
0.0
1E-8
1E-7
1E-6
1E-5
1E-4
Current density, A/cm2
PTFE coated sample
uncoated sample

Table 1 Material samples

Material	Grade	Sample Name	
		Uncoated	CoBlast PTFE Coated
Stainless Steel	316 L	SS316L	CSS316L
	304	SS304	CSS304
Titanium	G2	TiG2	CTiG2

Table 2 Mean values of three reading for roughness of uncoated and coated samples. Standard deviation is indicted below the values

Roughness Parameters (µm)	SS316L	CSS316L	SS304	CSS304	TiG2	CTiG2
Ra	0.199 ± 0.029	1.744 ±0.052	0.092 ±0.021	1.635 ±0.086	0.353 ±0.023	1.969 ±0.123
Rq	0.252 ±0.034	2.184 ±0.076	0.146 ±0.076	2.059 ±0.028	0.442 ±0.019	2.478 ±0.157

Table 3: Corrosion parameters of coated and uncoated samples in the simulated cathode and anode PEMFC environment

Material	Cathode		Anode	
	E_{corr} (V vs Ag/AgCl)	I_{corr} (µA/cm^2)	E_{corr} (V vs Ag/AgCl)	I_{corr} (µA/cm^2)
CSS316L	0.204	1.48	0.08	8.70
SS316L	0.007	4.13	-0.178	49.2
CSS304	-0.115	10	0.157	3.46
SS304	-0.1769	53.8	-0.25	60.1
CTiG2	0.13	413.0	0.121	6.84
TiG2	0.11	20.4	0.002	63.5